Presented at GNSS 2004
The 2004 International Symposium on GNSS/GPS

Sydney, Australia
6–8 December 2004

SLAM aided GPS/INS Navigation in GPS Denied and Unknown Environments

Jonghyuk Kim
ARC Centre of Excellence for Autonomous Systems, The University of Sydney, Australia
Tel: +61 (0)2 9351 8515, Fax: +61 (0)2 9351 7474, Email: jhkim@acfr.usyd.edu.au

Salah Sukkarieh
ARC Centre of Excellence for Autonomous Systems, The University of Sydney, Australia
Tel: +61 (0)2 9351 7515, Fax: +61 (0)2 9351 7474, Email: salah@acfr.usyd.edu.au

ABSTRACT

This paper presents the results of augmenting a GPS/INS navigation system with a Simultaneous Localisation and Mapping (SLAM). SLAM algorithm is a landmark based terrain aided navigation system that has the capability for online map building, and simultaneously utilising the generated map to bound the errors in the Inertial Navigation System (INS). Due to the low quality of the inertial sensors used, even a short-term GPS dropout can degrade the inertial navigation performance significantly, which can affect the vehicle safety as well. In addition, in GPS denied environments, most navigation systems need a separate aiding source in order to increase the reliability and availability. In this paper, SLAM is augmented to GPS/INS system, which can provide information about the states of a vehicle without the need for a priori infrastructure such as GPS, ground beacons, or a preloaded map. If GPS information is available, the SLAM integrated system builds a landmark-based map using a GPS/INS solution. If GPS is not available, the previously and/or newly generated map is used to constrain the INS errors. Simulation results will be presented which shows that the system can provide reliable and accurate navigation/landmark-map solutions even in a GPS denied and/or unknown environments.

KEYWORDS: Simultaneous Localisation and Mapping (SLAM), GPS/INS navigation, mapping and tracking, UAV.

1. INTRODUCTION

The Global Navigation Satellite System (GNSS) is a space-borne, radio navigation system. Its world-wide coverage, availability, and high accuracy make it one of history's most revolutionary developments. In airborne navigation, its complementary characteristics to the Inertial Navigation System (INS) make it an excellent aiding source and lead to extensive theoretical and practical research activities focussing on the fusion of Global Positioning

System (GPS) and INS to improve the accuracy and reduce the cost of navigation systems. The synergistic effects in the GPS/INS integrated system are well reported in many studies of Greenspan, 1996, Phillips and Schmidt, 1996, Kim and Sukkarieh, 2002, and etc. The current trends are incorporating a lower cost, or equivalently lower quality, inertial sensor with a higher performance GNSS sensor with deeply-coupled integration structures (Phillips and Schmidt, 1996). The low-cost, light, and compact-sized GPS/INS system is an ideal navigation system for the UAV platform, which has only a limited payload capacity and also requires high manoeuvrability to meet specific missions as well as precise navigation for autonomous operation.

The main drawback in the cost-effective GPS/INS system is that the integrated system becomes more dependent on the availability and quality of GNSS information. However GNSS information which relies on external satellite signals can be easily blocked or jammed by intentional/unintentional interference. Even a short duration of satellite signal blockage can cause signification deviation in navigation solution. Hence, research into Terrain Aided Navigation System (TANS) which can relieve the dependency on GNSS has been an active area (Baker and Clem, 1977, Hostetler and Andreas, 1983, Pritchett and Pue, 2000, Williams and et al, 2001). This type of navigation system typically makes use of onboard sensors and a preloaded terrain database. Terrain Contour Matching (TERCOM) system has been successfully applied in cruise missile navigation (Baker and Clem, 1977). In TANS, the DTE is the key element. However it usually requires some sort of space-borne or air-borne mapping infrastructure as it is typically built from high resolution satellite radar images around the mission area. Furthermore, it has a constrained degree of autonomy since the mission is bound to the knowledge of the terrain database.

In this paper, a new concept of terrain-aided navigation, known as Simultaneous Localisation and Mapping (SLAM) is augmented into the existing GPS/INS system. It was firstly addressed in the paper by Smith and Cheeseman, 1987 and has evolved from the indoor robotics research community to explore unknown environments, where absolute information is not available (Dissanayake and *et al*, 2001, Guivant and Nebot, 2001). Contrary to TANS, SLAM does not require any pre-surveyed map database. It builds the map incrementally by sensing environment and uses the map to localise the vehicle simultaneously, which results in a truly self-contained autonomous system.

The airborne 6DoF SLAM algorithm was firstly demonstrated in the paper by Kim and Sukkarieh, 2004. It can be described as shown in Figure 1. The vehicle starts its navigation at an unknown location in an unknown environment. The vehicle navigates using its dead-reckoning sensor or vehicle model. As the onboard sensors detect landmarks from the environment, the SLAM estimator augments the landmark locations to a map in some global reference frame and begins to estimate the vehicle and map states together with successive observations. The ability to estimate both the vehicle location and the map is due to the statistical correlations that exist within the estimator between the vehicle and landmarks, and between the landmarks themselves. As the vehicle proceeds through the environment and re-observes old landmarks, the map accuracy converges to a lower limit which is a function of the initial vehicle uncertainty when the first landmark was observed (Dissanayake and *et al*, 2001). In addition, the vehicle uncertainty is also constrained simultaneously.

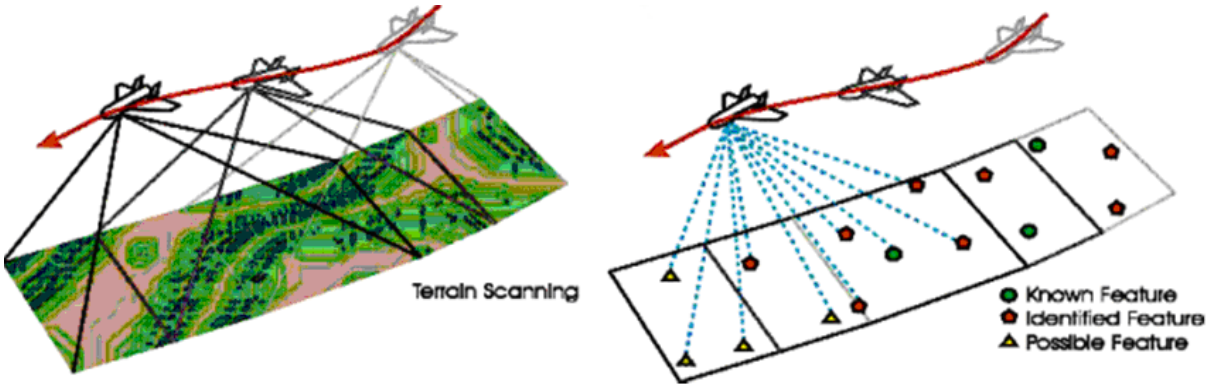

Figure 1. The overall structure of SLAM is about building a relative map of landmark-based landmarks using relative observations, defining a map, and using this map to localise the vehicle simultaneously.

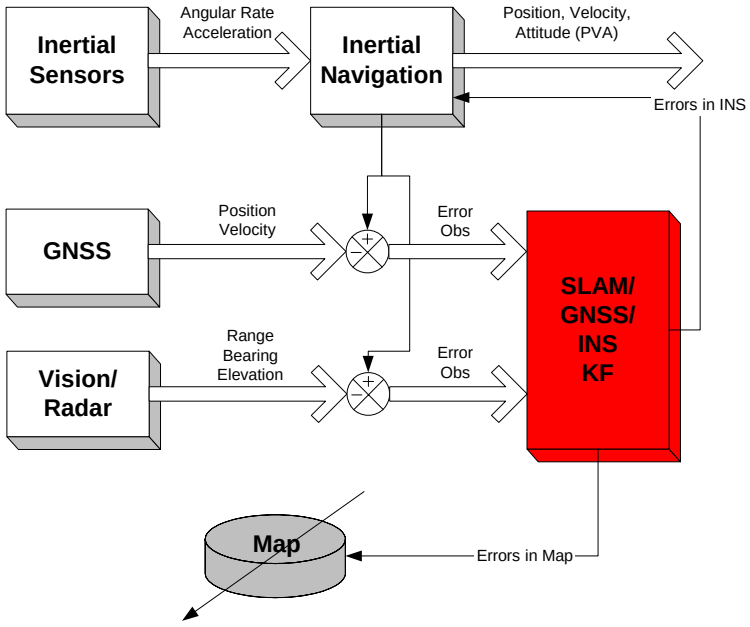

Figure 2. SLAM augmented GPS/INS system

In this paper the SLAM algorithm for a 6DoF platform is augmented to the GPS/INS navigation system to provide reliable INS aiding information in GNSS denied environment. Figure 2 presents the SLAM augmented GPS/INS architecture. The key landmark is the complementary fusion structure, which has high-speed INS module and low-speed and computationally expensive SLAM/GPS/INS filter. To achieve this, the SLAM algorithm was reformulated into error state form as in the work of Kim, 2004, which makes it to be easily augmented to GPS/INS filter.

In this architecture, the INS and map is maintained outside the SLAM filter and the map is treated as external map database. The fusion filter works as either landmark-tracking filter or SLAM filter depending on the availability of GNSS observation. If GNSS provides reliable observations, then the on-board vision or radar observations are used to build the landmark map and SLAM/GPS/INS filter estimates the errors in INS and map, which results in a

landmark (or target)-tracking system. However, in GNSS-denied situation, the vision or radar observations are solely used to estimate the errors in INS and map, which results in SLAM system. Although there are no global observations from GNSS, the constant re-observation and revisit processes can make the vehicle to navigate reliable within the map.

Section 2 will present the external INS loop and map and Section 3 will formulate the error model of SLAM/GPS/INS algorithm and Kalman filter structure. In Section 4, simulation results are provided based on our Brumby UAV, then Section 5 will provide conclusions and suggest future work.

2. EXTERNAL INS LOOP AND MAP

In the complementary SLAM/GPS/INS structure, the SLAM filter aids the external INS loop in a complementary fashion. The inertial navigation algorithm is to predict the high-dynamic vehicle states from the Inertial Measurement Unit (IMU) measurements. In this implementation a quaternion-based strapdown INS algorithm formulated in earth-fixed tangent frame is used (Kim, 2004):

$$\begin{bmatrix} \mathbf{p}^{\mathrm{n}}(k) \\ \mathbf{v}^{\mathrm{n}}(k) \\ \mathbf{q}^{\mathrm{n}}(k) \end{bmatrix} = \begin{bmatrix} \mathbf{p}^{\mathrm{n}}(k-1) + \mathbf{v}^{\mathrm{n}}(k-1)\Delta t \\ \mathbf{v}^{\mathrm{n}}(k-1) + [(\mathbf{q}^{\mathrm{n}}(k-1) \otimes \mathbf{f}^{\mathrm{b}}(k)) \otimes (\mathbf{q}^{\mathrm{n}})^{*}(k-1) + \mathbf{g}^{n}]\Delta t \\ \mathbf{q}^{\mathrm{n}}(k-1) \otimes \Delta\mathbf{q}^{\mathrm{n}}(k-1) \end{bmatrix} \tag{1}$$

where $\mathbf{p}^{n}(k), \mathbf{v}^{n}(k), \mathbf{q}^{n}(k)$ represent position, velocity, and quaternion respectively at discrete time k, Δt is the time for the position and velocity update interval, $(\mathbf{q}^{n})^{*}(k)$ is a quaternion conjugate for the vector transformation, $\otimes$ represents a quaternion multiplication, and $\Delta\mathbf{q}^{n}(k)$ is a delta quaternion computed from gyroscope readings during the attitude update interval (Kim, 2004).

A stationary landmark model is used with zero input disturbances. Hence the *i*-th landmark simply becomes,

$$\mathbf{m}_{i}^{n}(k) = \mathbf{m}_{i}^{n}(k-1) \tag{2}$$

If a new landmark is observed, this external map is dynamically augmented with the new landmark position, and the integrated SLAM filter covariance is also augmented with an initial uncertainty and correlation.

3. COMPLEMENTARY SLAM/GPS/INS ALGORITHM

The mathematical framework of the SLAM algorithm is based on an estimation process which, when given a kinematic/dynamic model of the vehicle and relative observations between the vehicle and landmarks, estimates the structure of the map and the vehicle's position, velocity and orientation within that map. In this work, the Kalman Filter (KF) is used as the state estimator.

3.1 Augmented Error State

In complementary SLAM, the state is now defined as the error state of vehicle and map:

$$\boldsymbol{\delta}\mathbf{x}(k) = [\boldsymbol{\delta}\mathbf{x}_v(k), \boldsymbol{\delta}\mathbf{x}_m(k)]^T \tag{3}$$

The error state of the vehicle $\boldsymbol{\delta}\mathbf{x}_v(k)$ comprises the errors in the INS indicated position, velocity and attitude expressed in the navigation frame:

$$\boldsymbol{\delta}\mathbf{x}_v(k) = [\boldsymbol{\delta}\mathbf{p}^n(k), \boldsymbol{\delta}\mathbf{v}^n(k), \boldsymbol{\delta}\boldsymbol{\psi}^n(k)]^T \tag{4}$$

The error state of the map $\boldsymbol{\delta}\mathbf{x}_m(k)$ also comprises the errors in 3D landmark positions in the navigation frame. The size of state is also dynamically augmented with the new landmark error after the initialisation process,

$$\boldsymbol{\delta}\mathbf{x}_m(k) = [\boldsymbol{\delta}\mathbf{m}_1^n(k), \boldsymbol{\delta}\mathbf{m}_2^n(k), \quad , \boldsymbol{\delta}\mathbf{m}_N^n(k)]^T , \tag{5}$$

where N is the current number of registered landmarks in the filter and each state consists of a 3D position error.

3.2 SLAM Error Model

The linearised SLAM system in discrete time can be written as

$$\boldsymbol{\delta}\mathbf{x}(k+1) = \mathbf{F}(k)\boldsymbol{\delta}\mathbf{x}(k) + \mathbf{G}(k)\mathbf{w}(k) \tag{6}$$

where $\boldsymbol{\delta}\mathbf{x}(k)$ is the error state vector, $\mathbf{F}(k)$ is the system transition matrix, $\mathbf{G}(k)$ is the system noise input matrix and $\mathbf{w}(k)$ is the system noise vector which represents the instrument noise with any un-modelled errors with noise strength $\mathbf{Q}(k)$.

The continuous time SLAM/Inertial error model is based on misalignment angle dynamics and stationary landmark model which is a random constant (Kim, 2004):

$$\begin{bmatrix} \boldsymbol{\delta}\mathbf{p}^n \\ \boldsymbol{\delta}\mathbf{v}^n \\ \boldsymbol{\delta}\boldsymbol{\psi}^n \\ \hline \boldsymbol{\delta}\mathbf{m}_m^n \end{bmatrix} = \begin{bmatrix} \boldsymbol{\delta}\mathbf{v}^n \\ \mathbf{C}_b^n\mathbf{f}^b \times \boldsymbol{\delta}\boldsymbol{\psi}^n + \mathbf{C}_b^n\boldsymbol{\delta}\mathbf{f}^b \\ -\mathbf{C}_b^n\boldsymbol{\delta}\boldsymbol{\omega}^b \\ \hline \mathbf{0}_m \end{bmatrix}, \tag{7}$$

where $\mathbf{f}^b$ and $\boldsymbol{\omega}^b$ are acceleration and rotation rates measured from IMU, $\boldsymbol{\delta}\mathbf{f}^b$ and $\boldsymbol{\delta}\boldsymbol{\omega}^b$ are the associated errors in IMU measurement, $\mathbf{C}_b^n$ is the direction cosine matrix formed from the quaternion. The discrete-time model can now be obtained by expanding the exponential state transition function and approximating it to the first-order term, and integrating the noise input during discrete sample time (Δt), which result in,

$$\mathbf{F}(k)=\left[\begin{array}{cccc} \mathbf{I} & \Delta t\mathbf{f}^n & \mathbf{0} & \mathbf{0} \\ \mathbf{0} & \mathbf{I} & \Delta t\mathbf{f}^n & \mathbf{0} \\ \mathbf{0} & \mathbf{0} & \mathbf{I} & \mathbf{0} \\ \hline \mathbf{0} & \mathbf{0} & \mathbf{0} & \mathbf{I}_{m\times m} \end{array}\right],\ \mathbf{G}(k)=\left[\begin{array}{cc} \mathbf{0} & \mathbf{0} \\ \sqrt{\Delta t}\mathbf{C}_b^n(k) & \mathbf{0} \\ \mathbf{0} & -\sqrt{\Delta t}\mathbf{C}_b^n(k) \\ \hline \mathbf{0}_m & \mathbf{0}_m \end{array}\right],\mathbf{Q}(k)=\left[\begin{array}{cc} \boldsymbol{\sigma}_{\delta f}^2 & \mathbf{0} \\ \mathbf{0} & \boldsymbol{\sigma}_{\delta\omega}^2 \end{array}\right] \quad (8)$$

with $\boldsymbol{\sigma}_{\delta f}$ and $\boldsymbol{\sigma}_{\delta\omega}$ representing noise strengths of acceleration and rotation rate respectively.

3.3 Observation model

The linearised observation model can be obtained in terms of the observation residual, or measurement differences, $\boldsymbol{\delta}\mathbf{z}(k)$ and the error states, $\boldsymbol{\delta}\mathbf{x}(k)$,

$$\boldsymbol{\delta}\mathbf{z}(k) = \mathbf{H}(k)\boldsymbol{\delta}\mathbf{x}(k) + \mathbf{v}(k) \quad (9)$$

with $\mathbf{H}(k)$ being the linearised observation Jacobian and $\mathbf{v}(k)$ being the observation noise with noise strength matrix $\mathbf{R}(k)$. The error observations are generated by subtracting the measured quantity, $\mathbf{z}(k)$, from the INS predicted quantity $\hat{\mathbf{z}}(k)$:

$$\boldsymbol{\delta}\mathbf{z}(k) = \boldsymbol{\delta}\hat{\mathbf{z}}(k) - \boldsymbol{\delta}\mathbf{z}(k). \quad (10)$$

As there are two different types of observation in this system, that is a range/bearing/elevation observation and a GNSS position/velocity observation, they should be formulated separately.

3.3.1 Range/Bearing/Elevation observation

In range/bearing/elevation observation, the onboard sensor provides relative observations between vehicle and landmarks. The non-linear observation equation relates these observations to the state as

$$\mathbf{z}(k) = \mathbf{h}(\mathbf{x}(k), \mathbf{v}(k)), \quad (11)$$

where $\mathbf{h}(\cdot)$ is the non-linear observation model at time k, and $\mathbf{v}(k)$ is the observation noise vector. Since the observation model predicts the range, bearing, and elevation for the i-th landmark, it is only a function of the i-th landmark and the vehicle state. Therefore Equation 8 can be further expressed as

$$\mathbf{z}_i(k) = \mathbf{h}(\mathbf{x}_v(k), \mathbf{x}_{mi}(k), \mathbf{v}_i(k)), \quad (12)$$

with $\mathbf{z}_i(k)$ and $\mathbf{v}_i(k)$ being the i-th observation and its associated additive noise in range, bearing and elevation with zero mean and variance of $\mathbf{R}(k)$. The landmark position in the navigation frame is initialised from the sensor observation in the sensor frame and vehicle state as shown in Figure 3.

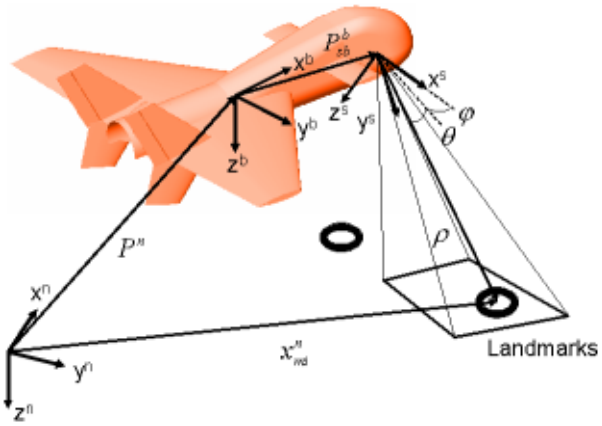

Figure 3. The range, bearing and elevation observations from the onboard sensor can be related to the location of the landmark in the navigation frame through the platform's position and attitude.

The initial landmark position in the navigation frame is then computed

$$\mathbf{m}_i^n(k) = \mathbf{p}^n(k) + \mathbf{C}_b^n(k)\mathbf{p}_{bs}^b + \mathbf{C}_b^n(k)\mathbf{C}_s^b\mathbf{p}_{sm}^s(k) \tag{13}$$

where $\mathbf{p}_{bs}^b(k)$ is the lever-arm offset of the sensor from the vehicle's centre of gravity in the body frame, $\mathbf{C}_s^b$ is a direction cosine matrix which transforms the vector in the sensor frame (such as camera instalment axes) to the body frame, and $\mathbf{p}_{sm}^s(k)$ is the relative position of the landmark from the sensor expressed in the sensor frame which is computed from the observation:

$$\mathbf{p}_{sm}^s(k) = \begin{bmatrix} \rho\cos(\varphi)\cos(\vartheta) \\ \rho\sin(\varphi)\cos(\vartheta) \\ \rho\sin(\vartheta) \end{bmatrix}, \tag{14}$$

with ρ, φ and ϑ being the range, bearing and elevation angle respectively, measured from the onboard sensor. Hence the predicted range, bearing and elevation between the vehicle and the *i*-th landmark in Equation 8 can now be obtained by rearranging Equation 10,

$$\mathbf{z}_i(k) \quad \begin{bmatrix} \rho \\ \varphi \\ \vartheta \end{bmatrix} = \begin{bmatrix} \sqrt{x^2+y^2+z^2} \\ \tan^{-1}(y/x) \\ \tan^{-1}(z/\sqrt{x^2+y^2}) \end{bmatrix}, \tag{15}$$

$$\text{with,} \begin{bmatrix} x \\ y \\ z \end{bmatrix} = \mathbf{p}_{sm}^s(k) = \mathbf{C}_b^s\mathbf{C}_n^b(k)[\mathbf{m}_i^n(k) - \mathbf{p}^n(k) - \mathbf{C}_b^n(k)\mathbf{p}_{bs}^b]. \tag{16}$$

The observation model is non-linear and has two composite functions; a coordinate transformation from the navigation frame to sensor frame, and transformation from Cartesian coordinates to polar coordinates. By calculating Jacobian of this equation, linearised discrete model is obtained:

$$\mathbf{H}(k) \begin{bmatrix} \frac{\partial \rho}{\partial \mathbf{p}^n} & \frac{\partial \rho}{\partial \mathbf{v}^n} & \frac{\partial \rho}{\partial \boldsymbol{\psi}^n} \\ \frac{\partial \varphi}{\partial \mathbf{p}^n} & \frac{\partial \varphi}{\partial \mathbf{v}^n} & \frac{\partial \varphi}{\partial \boldsymbol{\psi}^n} \\ \frac{\partial \vartheta}{\partial \mathbf{p}^n} & \frac{\partial \vartheta}{\partial \mathbf{v}^n} & \frac{\partial \vartheta}{\partial \boldsymbol{\psi}^n} \end{bmatrix}, \mathbf{R}(k) = \begin{bmatrix} \sigma_\rho^2 & 0 & 0 \\ 0 & \sigma_\varphi^2 & 0 \\ 0 & 0 & \sigma_\vartheta^2 \end{bmatrix}. \quad (17)$$

If vision or radar information is available, $\boldsymbol{\delta}\mathbf{z}(k)$ is formed by subtracting the range, bearing and elevation of the sensor from the INS indicated range, bearing and elevation, then it is fed to the integrated fusion filter to estimate the errors in vehicle and map.

3.3.2 GPS observation

GPS can provide several observables such as position/velocity, pseudorange/pseudorange-rate, or integrated carrier phase. If the position/velocity observation is used the observation model simply becomes a linear form with,

$$\mathbf{H}(k) \left[\begin{array}{ccc|c} \mathbf{I} & \mathbf{0} & \mathbf{0} & \mathbf{0}_m \\ \mathbf{0} & \mathbf{I} & \mathbf{0} & \mathbf{0}_m \end{array}\right], \mathbf{R}(k) = \begin{bmatrix} \boldsymbol{\sigma}_p^2 & \mathbf{0} \\ \mathbf{0} & \boldsymbol{\sigma}_v^2 \end{bmatrix}. \quad (18)$$

If GPS information is available, $\boldsymbol{\delta}\mathbf{z}(k)$ is formed by subtracting the position and velocity of the GPS from the INS indicated position and velocity, then they are fed to the fusion filter to estimate the errors in vehicle and map.

3.4 K/F Prediction

With the state transition and observation models defined in Equations 6 and 9, the estimation procedure can proceed. The state and its covariance are predicted using the process noise input. The state covariance is propagated using the state transition model and process noise matrix by,

$$\boldsymbol{\delta}\mathbf{x}(k \mid k-1) = \mathbf{F}(k)\delta\mathbf{x}(k-1 \mid k-1) = \mathbf{0} \quad (19)$$

$$\mathbf{P}(k \mid k-1) = \mathbf{F}(k)\mathbf{P}(k-1 \mid k-1)\mathbf{F}^T(k) + \mathbf{G}(k)\mathbf{Q}(k)\mathbf{G}^T(k) \quad (20)$$

Not only is the linear prediction much simpler and computationally more efficient than in the direct SLAM approach, but furthermore the predicted error estimate, $\boldsymbol{\delta}\mathbf{x}(k \mid k-1)$, is zero. This is because if one assumes that the only error in the vehicle and map states is zero mean Gaussian noise, then there is no error to propagate in the state prediction cycle, and the uncertainty in this assumption is provided in the covariance matrix propagation.

3.5 K/F Estimation

When an observation occurs, the state vector and its covariance are updated according to

$$\boldsymbol{\delta}\mathbf{x}(k \mid k) = \boldsymbol{\delta}\mathbf{x}(k \mid k-1) + \mathbf{W}(k)\mathbf{v}(k) = \mathbf{W}(k)\mathbf{v}(k) \tag{21}$$

$$\mathbf{P}(k \mid k) = \mathbf{P}(k \mid k-1) - \mathbf{W}(k)\mathbf{S}(k)\mathbf{W}^T(k) \tag{22}$$

where the innovation vector, Kalman weight, and innovation covariance are computed as,

$$\mathbf{v}(k) = \mathbf{z}(k) - \mathbf{H}(k)\delta\mathbf{x}(k \mid k-1) = \mathbf{z}(k) \tag{23}$$

$$\mathbf{W}(k) = \mathbf{P}(k \mid k-1)\mathbf{H}^T(k)\mathbf{S}^{-1}(k) \tag{24}$$

$$\mathbf{S}(k) = \mathbf{H}(k)\mathbf{P}(k \mid k-1)\mathbf{H}^T(k) + \mathbf{R}(k) \tag{25}$$

where, for the same reason as in the prediction cycle, $\mathbf{H}(k)\boldsymbol{\delta}\mathbf{x}(k \mid k-1)$ is zero and hence is not explicitly computed.

3.6 Feedback Error Correction

Once the observation estimation has been processed successfully, the estimated errors are now fed to the external INS loop and the map for correction. The corrected position, $\mathbf{p}_c^n(k)$, and velocity, $\mathbf{v}_c^n(k)$, are obtained by subtracting the estimated errors, and The corrected attitude quaternion, $\mathbf{q}_c^n(k)$, is obtained by pre-multiplying the error quaternion to the current quaternion:

$$\mathbf{p}_c^n(k) = \mathbf{p}^n(k) - \boldsymbol{\delta}\mathbf{p}^n(k \mid k) \tag{26}$$

$$\mathbf{v}_c^n(k) = \mathbf{v}^n(k) - \boldsymbol{\delta}\mathbf{v}^n(k \mid k) \tag{27}$$

$$\mathbf{q}_c^n(k) = \boldsymbol{\delta}\mathbf{q}^n(k) \otimes \mathbf{q}^n(k), \tag{28}$$

where the error quaternion $\boldsymbol{\delta}\mathbf{q}_c^n(k)$ is computed from the estimated misalignment angle:

$$\boldsymbol{\delta}\mathbf{q}^n(k) \cong \begin{bmatrix} 1 & \delta\psi_x/2 & \delta\psi_y/2 & \delta\psi_z/2 \end{bmatrix}^T \tag{29}$$

The corrected map positions are directly obtained by subtracting the estimated map position errors from the current positions:

$$(\mathbf{m}_N^n)_c(k) = \mathbf{m}_N^n(k) - \boldsymbol{\delta}\mathbf{m}_N^n(k \mid k) \tag{30}$$

Using these equations the complementary SLAM/GPS/INS Kalman filter can recursively fulfil its cycle of prediction and estimation with the external INS loop and the map.

3.6. Data Association and New landmark Augmentation

Data association is a process that finds out the correspondence between observations at time k and landmarks registered. Correct correspondence of the sensed landmark observations to mapped landmarks is essential for consistent map construction, and a single false match can invalidate the entire SLAM estimation process. Association validation is performed in observation space. As a statistical validation gate, the Normalised Innovation Square (NIS) is

used to associate observations. The NIS (γ) is computed by

$$\gamma = \mathbf{v}^T(k)\mathbf{S}^{-1}(k)\mathbf{v}(k) \tag{31}$$

Given an innovation and its covariance with the assumption of Gaussian distribution, γ forms a χ^2 (chi-square) distribution. If γ is less than a predefined threshold, then the observation and the landmark that were used to form the innovation are associated. The threshold value is obtained from the standard χ^2 tables and is chosen based on the confidence level required. Thus for example, a 99.5% confidence level, and for a state vector which includes three states of range, bearing, and elevation, then the threshold is 12.8. The associated innovation is now used to update the state and covariance. If the landmark is re-observed then the estimation cycle proceeds, otherwise it is a new landmark and must be augmented into both the external map and the covariance matrix (Kim, 2004).

4. RESULTS

A simulation analysis is performed to verify the proposed algorithm for the Brumby UAV, developed in University of Sydney, under GPS enabled and disabled scenarios.

4.1 Simulation Environment

A low-cost (or equivalently low quality) IMU is simulated with a vision as the range, bearing, and elevation sensor. The vision sensor used in the real system provides range information based on knowledge of target size; hence its range is simulated with large uncertainty. The simulation parameters obtained from the implemented actual sensor specifications are listed in Table I.

Sensor	Specification	Parameter
IMU	Sampling rate (Hz)	50
	Accel noise ($m/s^2/\sqrt{Hz}$)	0.5
	Gyro noise ($^\circ/s/\sqrt{Hz}$)	0.5
Vision	Frame rate (Hz)	25
	Field-Of-View ($^\circ$)	±15
	Estimated range error (m)	≥5
	Bearing noise ($^\circ$)	0.16
	Elevation noise ($^\circ$)	0.12
GPS	Position noise (m)	2.0
	Velocity noise (m/s)	0.5

Table 1. The parameters used in simulation

The flight vehicle undergoes three race-horse trajectories approximately 100m above the ground. The flight time is 460 seconds and the average flight speed is 40m/s. There are 80 landmarks placed on the ground. The vision observation is expressed in a camera frame which is transformed to navigation frame to be processed in the SLAM node. The biases of the IMU are calibrated precisely using onboard inclinometers in the real implementation thus the biases are not explicitly modelled and studied in the simulation analysis and only white noise is modelled as in Table 1.

4.2 GPS Active Region

Figure 4 shows the SLAM/GPS/INS estimated vehicle trajectory with the map built during the flight. The map uncertainty ellipsoids are also plotted with 10σ boundaries for the clarification. The vehicle takes off and flies over circuit-1 two rounds. It then transits to circuit-2 and circuit-3. To simulate GPS denied scenario, GPS signal is disabled between 130 to 420 seconds from the start.

After the vehicle taking off, GPS signal is available until 130 seconds. The SLAM/GPS/INS system behaves as a landmark-tracking/mapping system in this mode. The error covariance of landmarks around circuit-1 has relatively small value than landmarks around other circuits. Figure 7 presents the evolution of uncertainties of the vehicle and map. It can be clearly observed that the vehicle uncertainty was maintained within one metre until 130 seconds, and the uncertainties of observed landmarks are monotonically decreased. INS error is dominantly estimated from GPS information, and the GPS/INS blended navigation solution is used to track landmarks. Contrary to the conventional airborne mapping systems, SLAM/GPS/INS system maintains the cross-correlation information between the INS and map which can enhance the INS performance, and it is essential for the SLAM operation in GPS denied conditions.

4.3 GPS Denied Region

In this condition, the SLAM/GPS/INS system now behaves as a SLAM/INS system. INS and map errors are solely estimated from the landmark observation. The pre-registered landmark during GPS active period can be effectively used to estimate the INS and map errors as in Figures 5(a) and 5(c). More interesting SLAM property can be observed in Figures 5(b) and 5(d). After GPS is disabled, INS uncertainties begin to increase which in turn increases the registered map uncertainties. The accumulated INS error is effectively removed from the closing-the-loop effect, which, in turn, eliminates the INS error embodied in the map as shown in Figure 7. This is due to the correlation structure between vehicle and the map in SLAM. The map uncertainty decreases monotonically and whenever the vehicle observes the landmark, the vehicle error can be constrained effectively until GPS signal is available again. Figures 6(c) shows the final map uncertainties built in GPS enabled and disabled conditions.
When GPS signal is re-activated, the INS position and velocity errors are directly observed from the GPS measurements, which, in-turn, improves the map accuracy via the vehicle-map correlation structure within SLAM filter. From these plots, it is obvious that the SLAM/GPS/INS system can perform navigation and mapping for extended periods of time under GPS denied conditions

5. CONCLUSIONS

A new concept for the autonomous UAV navigation is presented based on the Simultaneous Localisation and Mapping (SLAM) algorithm, and applying it to a 6DoF airborne platform. The simulation analysis illustrates that the SLAM system with a range, bearing, and elevation sensor can constraint the INS errors effectively, performing on-line map building in unknown terrain environments. The SLAM augmented GPS/INS system shows two capabilities of landmark tracking and mapping using GPS information, and more importantly, aiding the INS under GPS denied situation. As a result, the SLAM augmented low-cost GPS/INS system can be effectively applied to various GPS denied situations, such as urban canyons, indoor, or

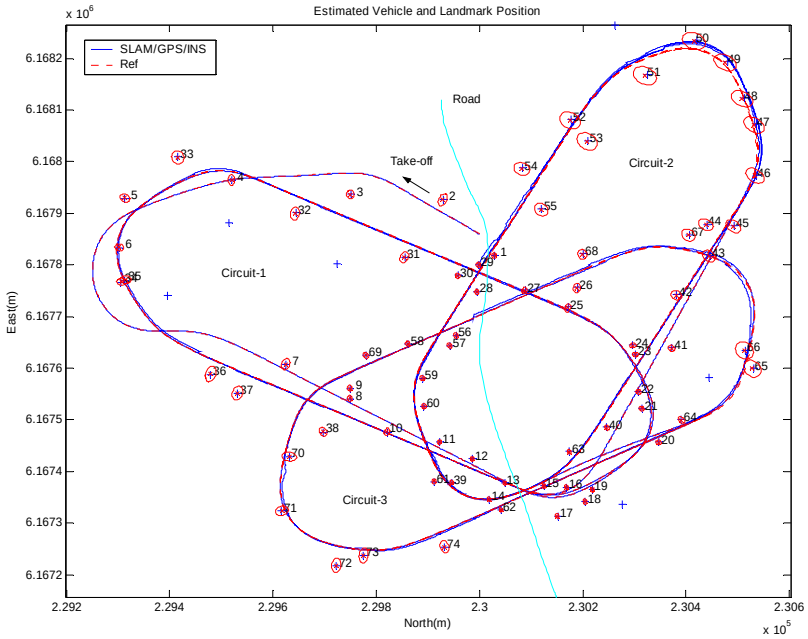

Figure 4. 2D position result of the SLAM augmented GPS/INS navigation. UAV takes off at (0,0) and flies three different race-horse tracks (circuit-1,2,3) in counter clock-wise. GPS signal is disabled in circuit-1 and re-enabled at the end of in circuit-3. The vision is abaliable during whole flight time which is used for feature-tracking and SLAM.

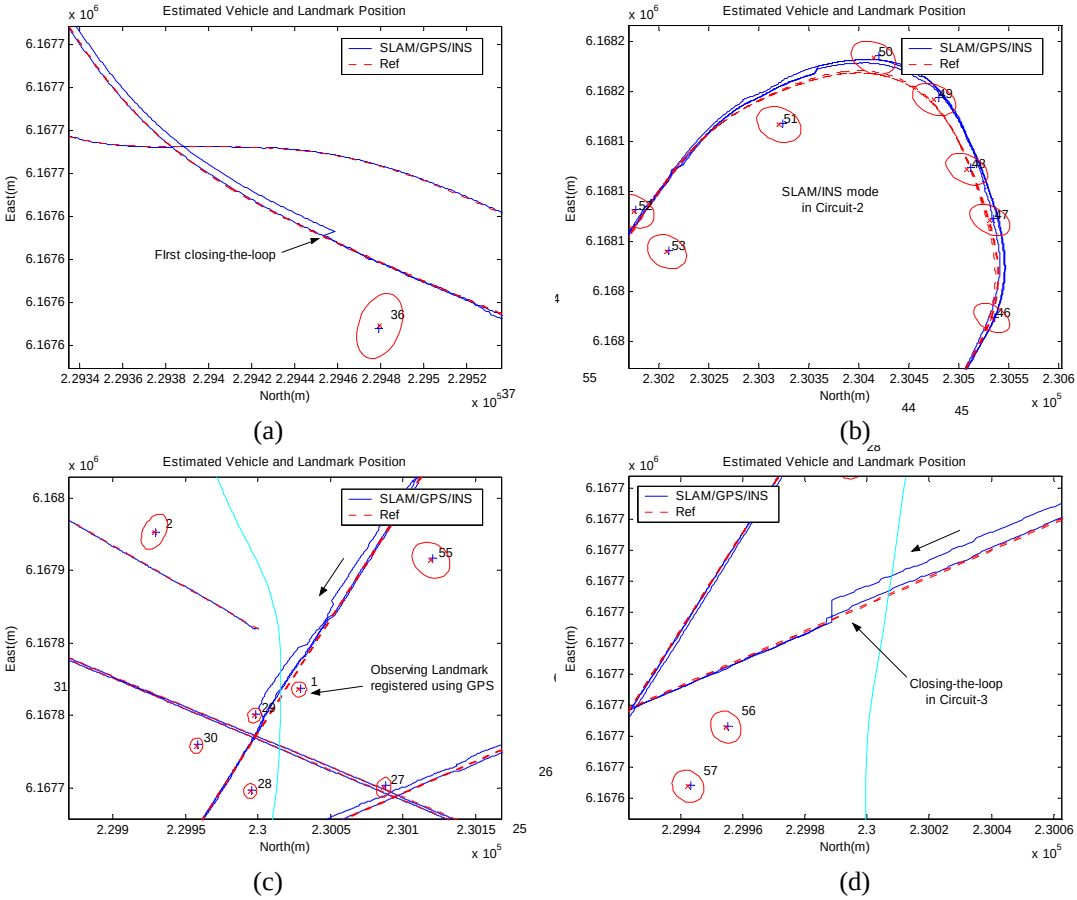

Figure 5. Enhanced view of SLAM aided INS navigation during GPS disabled condition.

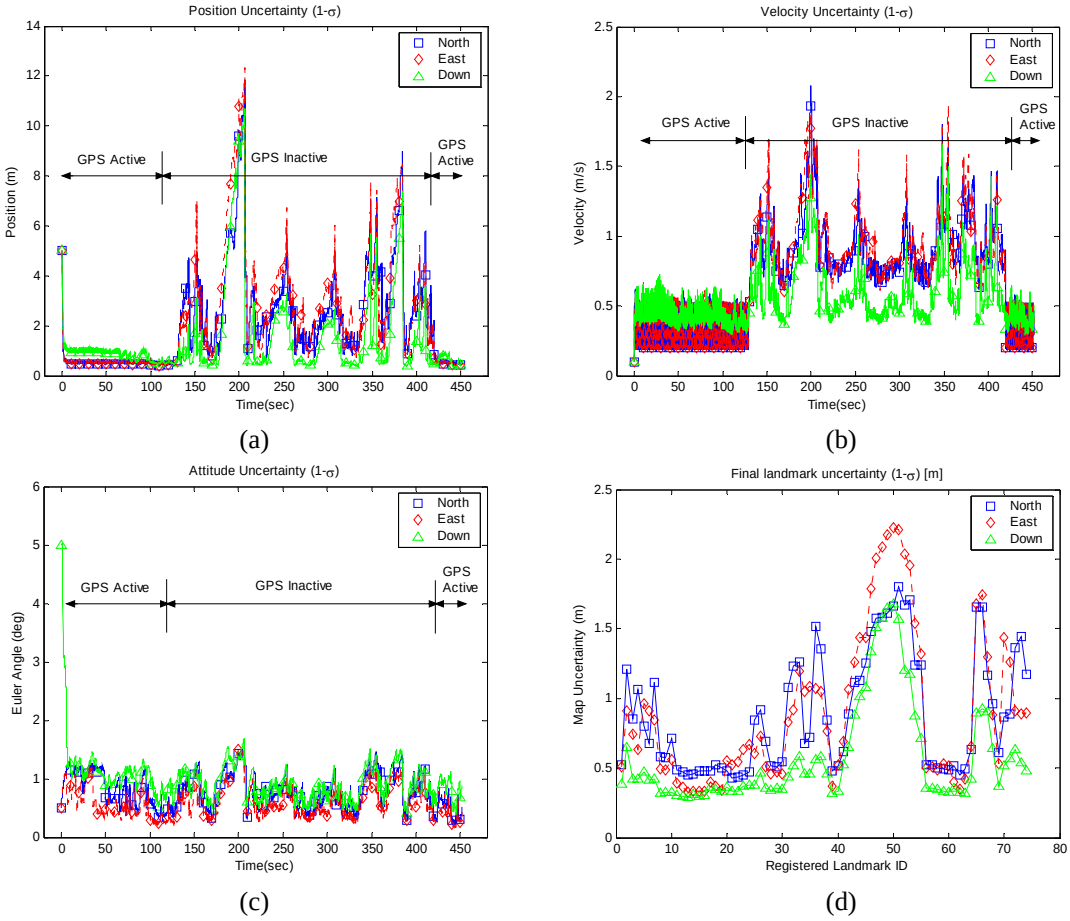

Figure 6. Covariance plot of the INS position (a), velocity (b), attitude (c) and final map (d). GPS is disabled at 130 second and re-enabled at 420 second.

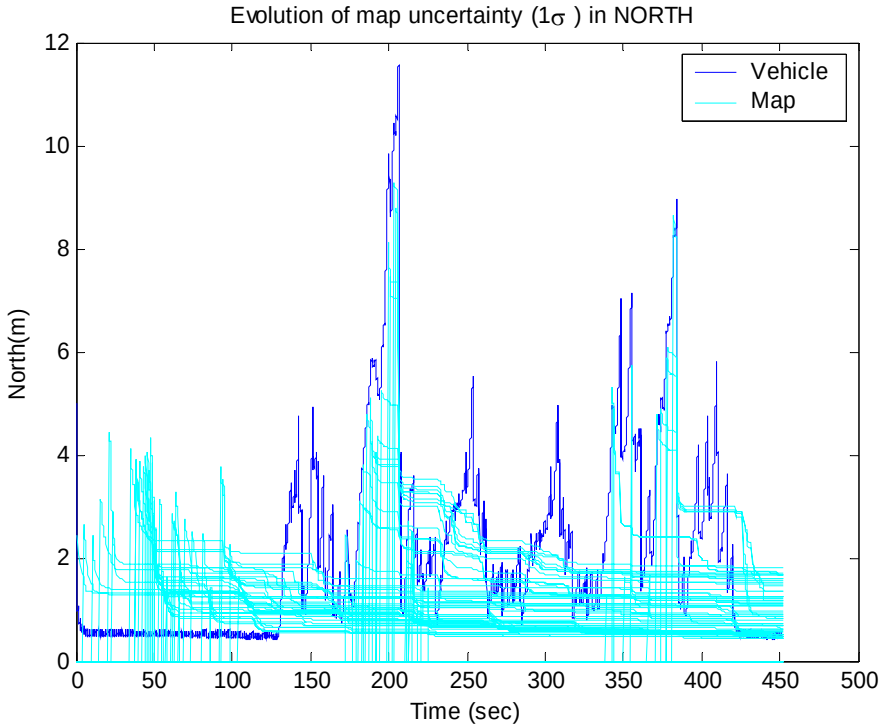

Figure 7. Covariance plot of the map and vehicle in the north position.

even underwater. The efficient map management for the large-scale SLAM and the real-time implementation in UAV platform using low-cost sensor are being tackled at the moment

ACKNOWLEDGEMENTS: This work is supported in part by the ARC Centre of Excellence programme, funded by the Australian Research Council (ARC) and the New South Wales State Government.

REFERENCES

Baker W.R. and Clem R.W. (1997) ***Terrain contour matching (TERCOM) premier***, ASP-TR-77-61. Aeronautical Systems Division, Wright-Patterson.

Dissanayake M.W.M.G., Newman P., Durrant-Whyte H., Clark S., and Csorba M. (2001) ***A solution to the simultaneous localization and map building problem,*** IEEE Transactions on Robotics and Automation, June, 17(3):229–241.

Guivant J. and Nebot E. (2001) ***Optimisations of the simultaneous localization and map building algorithm for real-time implementation***, IEEE Transactions on Robotics and Automation, 17(3):242–257.

Kim J. and Sukkarieh S. (2002) ***Flight Test Results of a GPS/INS Navigation Loop for an Autonomous Unmanned Aerial Vehicle (UAV),*** Proceedings of the 15th International Technical Meeting of the Satellite Division of the Institute of Navigation, September, OR, USA, 510–517.

Kim J. and Sukkarieh S. (2004) ***Autonomous Airborne Navigation in Unknown Terrain Environments,*** IEEE Transactions on Aerospace and Electronic Systems, 40(3):1031-1045, July

Kim J. (2004) ***Autonomous Navigation for Airborne Applications,*** PhD thesis, Australian Centre for Field Robotics, The University of Sydney.

Phillips R.E. and Schmidt G.T. (1996) ***GPS/INS Integration,*** In Advisory Group for Aerospace Research and Development (AGARD), Lecture series 207:9.1–9.10.

Smith R. and Cheeseman P. (1987) ***On the Representation of Spatial Uncertainty,*** In International Journal of Robotics Research, 5(4):56–68.

Williams S.B., Dissanayake M.W.M.G. and Durrant-Whyte H. (2001) ***Towards terrain-aided navigation for underwater robotics,*** In Advanced Robotics, 15(5):533–550.